Polyhedron 52 (2013) 1239–1245

Contents lists available at SciVerse ScienceDirect

Polyhedron

journal homepage: www.elsevier.com/locate/poly

First row transition metal complexes of a hexadentate pyrazole-based bispidine ligand

Peter Comba *, Michael Morgen, Hubert Wadepohl

Anorganisch-Chemisches Institut, Universität Heidelberg, Im Neuenheimer Feld 270, Heidelberg, Germany

ARTICLE INFO

Article history:
Available online 27 June 2012

Keywords:
Bispidine
Trigonal prismatic
Crystallography

ABSTRACT

The efficient synthesis of a new hexadentate pyrazole-based bispidine-ligand and its first-row transition metal complexes (Fe^{II}, Co^{II}, Ni^{II}, Cu^{II} and Zn^{II}) is reported. There are interesting structural differences between the present and earlier hexadentate bispidine ligands (tetragonally versus trigonally distorted octahedral geometries). The structural analysis of the metal-free ligand and the five complexes shows that the structure enforced by the rigid pyrazole-based bispidine is best described as distorted trigonal prismatic, and this also emerges from the spectroscopic analysis.

1. Introduction

Since Alfred Werner's discovery of coordination chemistry, octahedral structures are in the focus of transition metal coordination compounds. Smaller and larger coordination numbers and other geometries for six-coordinate complexes (trigonal prismatic versus trigonal antiprismatic) are known but less common – and often ignored [1]. Square planar, square pyramidal and square bipyramidal (octahedral) geometries satisfy the preferences exerted by the d-orbital set of the metal center but, for classical coordination compounds (i.e., relatively high oxidation states) ligand dictation is more important in terms of coordination geometries than the metal-ion-dependent electronic preferences [2–5].[1] That is, with a well chosen ligand system, "exotic" geometries may be enforced, and these may lead to specific and interesting stabilities, selectivities, reactivities and electronic properties [6]. Trigonal prismatic structures in solids have been described as early as 1923 [7], and for molecular compounds, trigonal prismatic structures have been predicted shortly afterwards [8] and discovered and discussed from the 1960s onwards [9,10]. Interestingly, the various models for their description and rationalization include pure geometric approaches, steric considerations, ligand-field-based models and molecular orbital descriptions [11–18]. Of interest is that with particular sets of first row transition metal hexamines, a ligand-field based analysis [19] and a molecular mechanics approach without any specific electronic effects included [20] lead to basically identical results, and this stresses the assertion that coordination geometries are largely enforced by the ligands, i.e., the metal-ion-based electronic forces are less important (see above) [1,2,21–25].[2] The trigonal twist of hexacoordinate complexes has had impact in various areas [11–18], and the probably most obvious feature is related to an isomerization pathway of chiral octahedral complexes, i.e., the Bailar twist [26].

Bispidines (3,7-diazabicyclo[3.3.1]nonane; see Scheme 1) are derived from the natural product sparteine and were first synthesized by Mannich [27]; first transition metal complexes have been reported in the 1950s [28,29]. As adamantane derivatives, these ligands are extremely rigid [30–32] and the specifically distorted *cis*-octahedral structures enforced have been shown to lead to a widely variable and unique coordination chemistry [33]. The bispidines are easily built-up by two consecutive double-Mannich reactions and therefore are highly flexible in terms of their design. By variation of the aldehyde- and/or amine-components a multitude of aromatic and aliphatic moieties with donor atoms ranging from nitrogen to oxygen and sulfur can be incorporated in the adamantane-like backbone [34]. In the original bispidine ligands (**L**^{1} in Scheme 1) the C2/C4 positions generally are substituted with aromatic nitrogen donors, and further donor groups, generally also pyridine moieties, are introduced at N3/N7 for the pentadentate and hexadentate ligands. This leads to square-pyramidal or *cis*-octahedral coordination geometries of their transition metal complexes (N^3, py^{C2}, py^{C4} and py^{N7} in equatorial position; py^{N3} and N7 in axial position). A second generation of bispidine ligands (e.g., **L**^{2} in Scheme 1) [35] may have exclusively aliphatic nitrogen donors which are introduced in the backbone by variation of the amine component at N3/N7. These ligands enforce trigonal

---

* Corresponding author.
E-mail address: peter.comba@aci.uni-heidelberg.de (P. Comba).

[1] Note that this is different for typical organometallic compounds with lower oxidation numbers, see Refs. [3–5].

[2] Note that there are electronically doped molecular mechanics approaches [20,21], and these lead to slightly more accurate structural predictions of the complex geometries. Note also that metal-ion based electronic effects clearly are of importance for thermodynamic effects, reactivities and spectroscopy [1,2,22,23].

0277-5387/$ - see front matter © 2012 Elsevier Ltd. All rights reserved.
http://dx.doi.org/10.1016/j.poly.2012.06.035

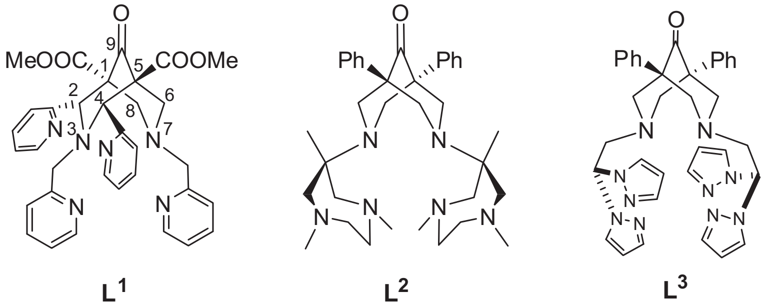

Scheme 1. Examples of a hexadentate first generation bispidine (left) which results in a tetragonally elongated octahedral coordination geometry, a hexadentate second generation bispidine which enforces a distorted trigonal prismatic geometry to transition metal ions (middle) and the new pyrazole-based bispidine ligand **L^3** (right).

geometries (distorted trigonal prismatic for the hexadentate ligand **L**^{2} and distorted trigonal bipyramidal for the corresponding tetra- and pentadentate ligands).

Bispidines of the first generation find broad applications, and this is due to their rigid structure and the coordination geometry enforced to the metal ion. In particular, for Cu^{II} this leads to high complex stabilities (e.g., with **L**^{1}, log $K^{Cu(II)}$ = 16.28; **L**^{2}, log $K^{Cu(II)}$ = 19.48) [35–37]. Together with relatively fast complexation processes (open-chain ligands) and the fact that there are functional groups which may be coupled to biomolecules (ester groups at C1/C5, carbonyl group at C9), these ligands have found application as bifunctional chelators for PET-imaging (positron emission tomography) [34]. In molecular catalysis, transition metal complexes of bispidines of the first generation are used, for example, in the Cu^{II}-catalyzed aziridination [38], and Fe^{II}-catalyzed sulfoxidation [39], olefin-oxidation [40], CH-hydroxylation [41] and halogenation reactions [42]. A common possibility to tune catalytic activity is by tuning the coordination geometry. However, due to the arrangement of the aromatic donors at C2/C4 distortion of the (pseudo)octahedral coordination geometry is limited. The development of rigid, well preorganized bispidines with different coordination geometries, e.g., trigonal instead of tetragonal, still is a demanding and valuable task.

We therefore present here a new ligand which is structurally related to **L**^{2} but has aromatic N-donors similar to **L**^{1}, i.e., the pyrazole-based bispidine ligand **L**^{3} with a bis-amine-tetrakis-pyrazole donor set, and discuss the corresponding structural and solution properties of first-row transition metal complexes with a special emphasis on the Cu^{II} systems.

2. Results and discussion

2.1. Ligand synthesis

The amine component **5** of the ligand was synthesized in a three-step procedure as reported before [43], starting from the aminoacetaldehyde dimethylacetal **1**, which is protected using 1,8-naphthalic acid anhydride **2**, followed by substitution of the methoxy groups with pyrazole, affording the protected dipyrazole-amine **4**. Finally, hydrazinolytic deprotection of **4** results in the free amine **5**. The ligand **L**^{3} was obtained in the usual way by a double Mannich reaction of 1,3-diphenyl-2-propanone, paraformaldehyde, the amine **5** and acetic acid as reagent, in refluxing ethanol (Scheme 2).

A crystal structure of the ligand **L**^{3} reveals that the most stable form is the boat–chair conformer, as expected due to the size of the amine substituents and the electron pair repulsion, emerging from the nitrogen atoms N3 and N7 in the hypothetical chair–chair conformation of the bispidine backbone (Fig. 1) [33]. However, in the presence of a metal ion, the bispidine backbone easily adopts the required chair–chair conformation. Complexes of divalent first-row transition metal ions were obtained by stirring equimolar mixtures of **L**^{3} and the corresponding metal salts (as perchlorates or tetrafluoroborates) in acetonitrile over night. Pure samples and crystals for X-ray crystallography were isolated by ether diffusion (Fig. 2).

2.2. Coordination chemistry

There are significant differences in the transition metal coordination chemistry between the 1st and 2nd generation bispidine ligands, in particular also with Cu^{II}. With the tetradentate ligands, the 1st generation bispidines form very stable end-on-peroxo-dicopper(II) complexes [30,44,45] and lead to interesting catecholase model compounds [46–48], while the 2nd generation bispidine-copper(I) complexes with dioxygen lead to the reversible formation of mononuclear superoxo complexes [49]. Also, there is a striking difference in the copper-catalyzed aziridination in terms of efficiency and reaction pathway, and this has been shown to be related to a large extent to differences in redox potentials [35,38,50,51]. Due to a ligand-enforced tetragonal distortion of the complexes with both types of bispidine ligands the Cu^{II} complexes are particularly stable and, together with the fast complex formation (non-cyclic ligands) and an efficient shielding of the metal centers by the hexadentate derivatives, these are potent ligands for radiopharmaceutical applications [35–37,52]. The significantly different stability constants between [Cu**L**^{1}]$^{2+}$ and [Cu**L**^{2}]$^{2+}$ (about three orders of magnitude) are also related to the corresponding redox potentials [35,37,53], and this must be due to the different coordination geometry, combined with differences in donor sets. We anticipated that the **L**^{2}- and **L**^{3}-based complexes might have very similar coordination geometries, and the differences in donor sets should then be the major factor to influence the complex stabilities as well as the redox potentials and ligand field transitions. The relative basicities (pK_a-values (conjugate acids): tertiary amines, ≈10; pyridine, 5.2 (2-methylpyridine: 6.0); 1H-imidazole, 7.0; 1-methylimidazole, 7.0; 1H-pyrazole 2.5) [54] and the ligand-field parameters (e_σ, e_π [cm^{-1}]; tertiary amine, 7100, 0; pyridine, 6200, 930; pyrazole, 5200, 700) [55–57])[3] lead to the expectation that the stabilities of the **L**^{2}- and **L**^{3}-based complexes must be very similar, and the coordination geometry therefore plays a major role.

The coordination geometry and d-orbital splitting of **L**^{3}-based complexes are described in Scheme 3; each trigonal plane consists of one of the tertiary amines from the bispidine backbone (N3 or

---

[3] Note that these are estimates based on a normalization to a reference Cu–N distance of 2.03 Å [56].

[4] Angle between a donor atom of one trigonal plane, the metal centre and the projection of the closest donor atom of the opposite trigonal plane; the twist angle Φ of an ideal trigonal prism is 0° that of an ideal octahedron is 60 °C.

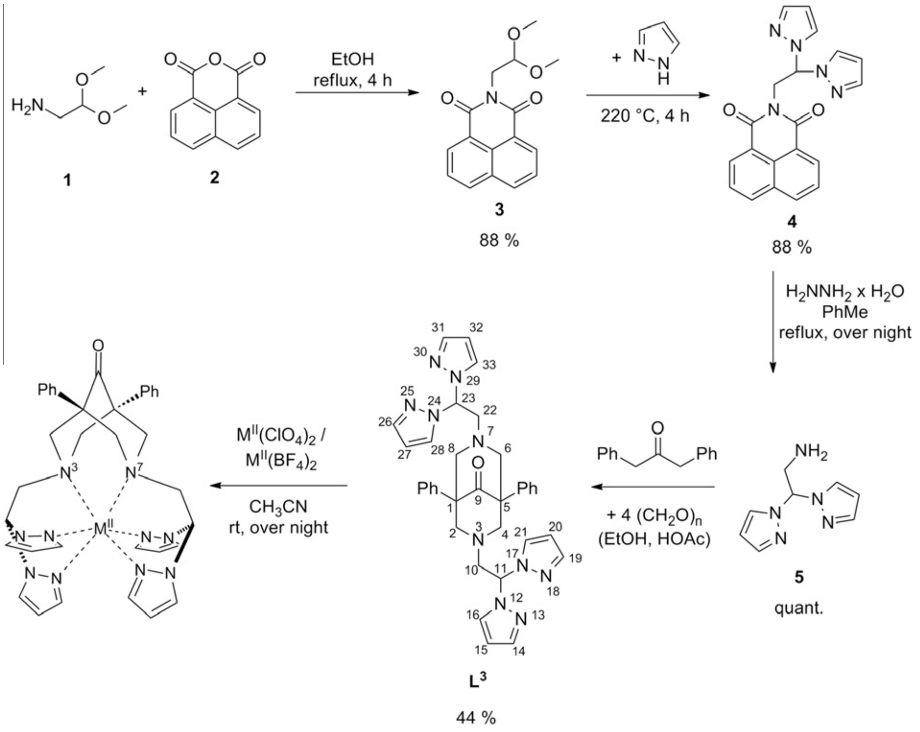

Scheme 2. Synthesis of the hexadentate pyrazole-based bispidine-ligand $\mathbf{L}^3$ and its corresponding metal complexes.

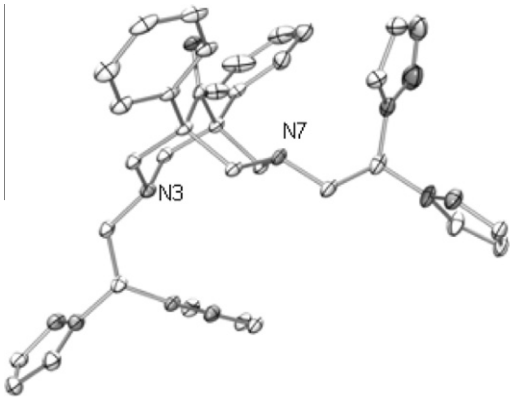

Fig. 1. ORTEP plot of the experimental structure of the metal-free ligand $\mathbf{L}^3$. Ellipsoids are shown at a 30% probability level. H atoms are omitted for clarity.

N7) and the two appended pyrazolyl donors (N13, N18 or N25, N30, respectively). The two corresponding trigonal planes are almost parallel with $\Theta = 1.83°$ (for Fe^{II}) – 8.51° (for Cu^{II}), and the inter-plane distance of 2.8–2.9 Å, is dictated by the rigid bispidine backbone (distance of the donor atoms N3 and N7; see Fig. 2 for plots of the experimental structures and Table 1 for the corresponding structural parameters). The trigonal twist angles[4] are between 15° and 20° for the N3···N7 edge but between 35° and 41° on average. That is, the complexes are best described as distorted trigonal prismatic, and this is as expected (see above), a very similar situation to that with the ligand $\mathbf{L}^2$ with only tertiary amine donors and a very similar backbone (note that the twist angles with $\mathbf{L}^2$ are very similar but the trigonal planes are significantly more parallel with $\mathbf{L}^3$) [35]. It appears that the $\mathbf{L}^3$-based complexes are less strained due to the fact that the pyrazole groups are free to rotate while the aliphatic nitrogen donors of $\mathbf{L}^2$ are fixed in a diazepane ring. However, the twist angles are slightly larger due to repulsion of the pyrazole H-atoms.

As expected from the structural properties, the e′ set of orbitals is nearly degenerate with a_1' and, at least for Cu^{II}, due to the Jahn–Teller instability and the ligand-enforced tetragonal distortion (see Table 1 and Fig. 2) [35], there is a significant splitting of the e″ set of orbitals. As a result, for Cu^{II} a d_{z^2} ground state is expected, and this clearly emerges from the corresponding EPR spectrum (Fig. 3); the spin Hamiltonian parameters for $[Cu\mathbf{L}^2]^{2+}$ and $[Cu\mathbf{L}^3]^{2+}$ indicate that the two copper(II) complexes have very similar ground states. This also emerges from the ligand field spectra (see Table 2). Based on the basicities and ligand field parameters (see above), a slightly lower ligand field might have been expected for $[Cu\mathbf{L}^3]^{2+}$ but the significantly higher symmetry and slightly more octahedral geometry as well as slightly smaller bond distances all lead to an increasing ligand field.

Unfortunately, only irreversible reduction signals are observed in cyclovoltammetric experiments. The $\mathbf{L}^3$-based Cu^{II} complex shows a peak at $E_p = -245$ mV (versus Fc/Fc^+ in MeCN, see Supporting Information). The corresponding $\mathbf{L}^1$- and $\mathbf{L}^2$-based complexes have reversible potentials and, importantly, these are at much more negative potentials. As mentioned in the Introduction, bispidine ligands, in particular those of the 1st generation, lead to very stable Cu^{II} complexes [37]. Interestingly, the redox potentials of Cu^{II} complexes are correlated to the complex stabilities [53]. While general correlations of this type should not be expected, the two groups of 1st and 2nd generation bispidine-copper complexes have been shown to lead to rather good linear dependencies of the $Cu^{II/I}$ couples with the $\log K^{Cu(II)}$ values.

Therefore, $\mathbf{L}^3$ forms less stable Cu^{II} complexes than the corresponding 1st generation bispidine ligands, and this is due to (i) a less preferential geometry (distorted trigonal prismatic versus distorted *cis*-octahedral), and to (ii) the lower basicity of the aromatic nitrogen donor ($pK_a = 2.5$ of 1H-pyrazole and $pK_a = 5.2$ of pyridine).

---

[4] Angle between a donor atom of one trigonal plane, the metal centre and the projection of the closest donor atom of the opposite trigonal plane; the twist angle Φ of an ideal trigonal prism is 0° that of an ideal octahedron is 60 °C.

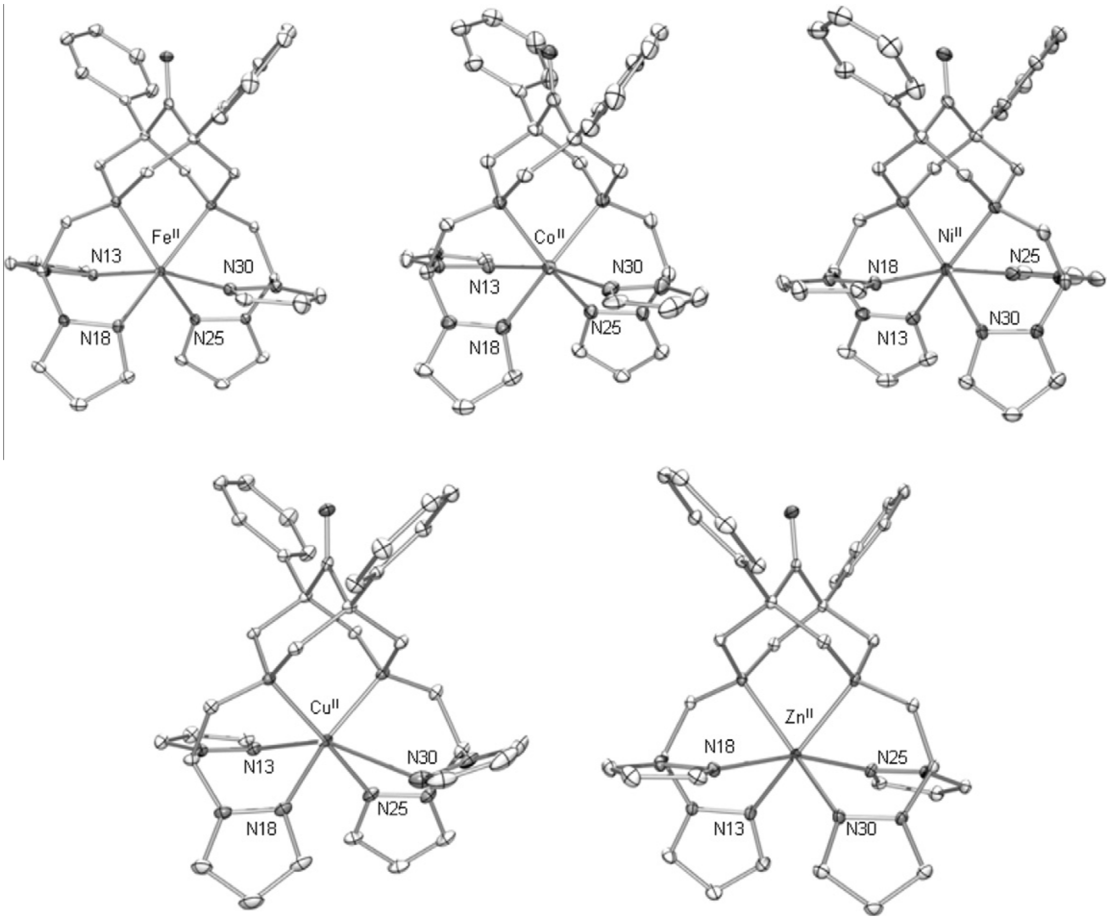

Fig. 2. ORTEP plots of the experimental structures of the M^{II}-complexes with the pyrazole-based bispidine $\mathbf{L}^3$. Ellipsoids are shown at a 30% probability level; counter ions, solvent molecules and H atoms are omitted for clarity (for numbering see also Scheme 2).

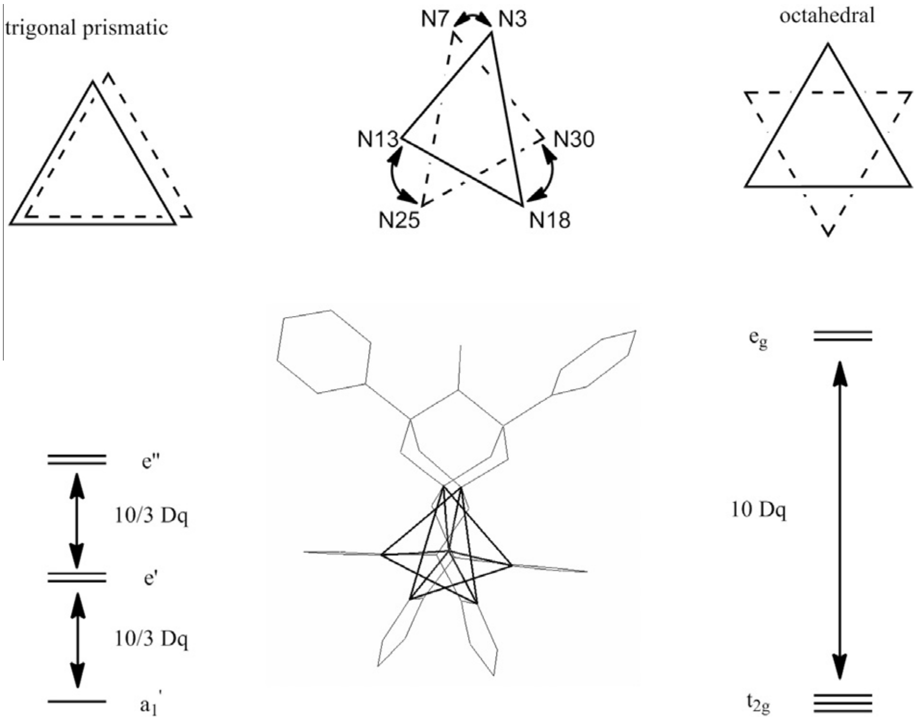

Scheme 3. Presentation of an ideal trigonal prism (left), an ideal octahedron (right) and the corresponding d-orbital-splitting; the coordination geometry of metal complexes with $\mathbf{L}^3$ are also shown (middle).

Table 1
Selected bond distances (Å) and angles (°) of the divalent transition metal-complexes with $\mathbf{L}^3$ (top), angles between the trigonal planes Θ and trigonal twist angles Φ (bottom).

M	M–N3	M–N7	M–N13	M–N18	M–N25	M–N30	N3···N7	N3–M–N30	N7–M–N13	N18–M–N25	N3–M–N7	N3–M–N13	N13–M–N30	N30–M–N7
Fe^{II}	2.252(2)	2.258(2)	2.166(2)	2.153(2)	2.148(2)	2.179(2)	2.834	110.47(7)	112.92(7)	102.79(7)	77.85(6)	80.67(6)	165.18(7)	79.77(7)
Co^{II}	2.214(3)	2.219(3)	2.131(3)	2.111(3)	2.104(3)	2.137(3)	2.826	108.79(11)	112.72(11)	101.13(11)	79.20(10)	80.34(10)	166.14(11)	79.81(11)
Ni^{II}	2.166(4)	2.180(4)	2.083(4)	2.108(4)	2.103(4)	2.077(4)	2.806	164.76(16)	163.36(16)	167.27(16)	80.44(15)	94.78(16)	94.14(17)	94.20(15)
Cu^{II}	2.065(2)	2.055(2)	2.301(2)	2.015(2)	1.992(2)	2.774(3)	2.815	116.40(8)	117.16(7)	91.12(8)	86.19(7)	82.85(7)	156.56(6)	79.29(7)
Zn^{II}	2.201(2)	2.231(2)	2.117(2)	2.232(2)	2.201(2)	2.101(2)	2.856	157.37(7)	161.30(6)	162.64(6)	80.23(6)	93.10(6)	101.14(7)	90.96(6)

	Θ	Φ_1 (N3/N7)	Φ_2 (N13/N25)	Φ_3 (N18/N30)	Φ_{av}
Fe^{II}	1.83	20.17	44.46	43.03	35.89
Co^{II}	4.07	20.43	47.82	43.76	37.34
Ni^{II}	5.08	23.74	48.26	52.38	41.46
Cu^{II}	8.51	15.10	57.58	38.73	37.14
Zn^{II}	3.51	18.65	43.64	42.81	35.03

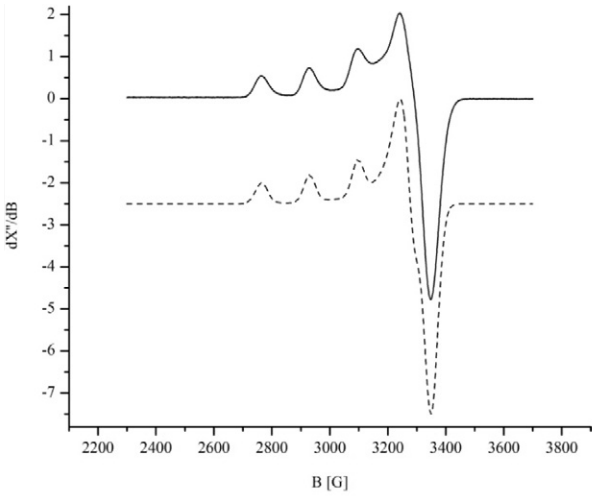

Fig. 3. EPR-spectrum of $[Cu^{II}\mathbf{L}^3][BF_4]_2$. Experimental spectrum measured in MeOH at 110 K, at a frequency of 9.453599 GHz (solid line), simulated spectrum ($g_{x,y} = 2.061$, $g_z = 2.241$, $A_{x,y} = 12$ G, $A_z = 170$ G) (dashed line) [58,59].

3. Experimental

3.1. Materials and methods

Chemicals were purchased from Sigma–Aldrich Chemie GmbH (Taufkirchen, Germany), ABCR GmbH & Co. KG (Karlsruhe, Germany) and Merck KGaA (Darmstadt, Germany) and were of the highest available purity. Dry solvents were used as delivered without further purification. NMR spectra were recorded on a Bruker DRX 200, Bruker Avance II 400 or Bruker Avance III 600 spectrometer. The latter spectrometer was equipped with a direct detection cryoprobe for maximum sensitivity in the detection of ^{13}C. ^{1}H and ^{13}C NMR chemical shifts were referenced to the signals of the solvent ($CDCl_3$). Mass spectra were recorded on a Finnigan MAT8230 and a Joel JMS-700 spectrometer. Elemental analyses were performed on a CHN-O-vario EL by the "Mikroanalytische Labor", Department of Organic Chemistry, University of Heidelberg. The electrochemical measurements were performed on CH Instruments CHI660D electrochemical workstation (equipped with a CH Instruments Picoamp Booster and Faraday Cage) with a three-electrode setup consisting of a glassy-carbon working electrode, a Pt wire as the auxiliary electrode and an Ag/$AgNO_3$ reference electrode (0.01 M Ag^+, 0.1 M $(Bu_4N)(BF_4)$ in MeCN). The solutions were thoroughly degassed and a slight argon-stream was set above the solution during the measurement; a scan rate of 100 mV s^{-1} was applied. UV–Vis-spectra were recorded on a Jasco V-570 UV–Vis-near-IR spectrophotometer. Solution spectra were measured from *in situ*-prepared complexes. For solid state UV–Vis-spectra the isolated complexes were triturated with titanium(IV)oxide. EPR measurements were performed on a Bruker ELEXSYS-E-500 instrument at 110 K using methanol as solvent. The spin Hamiltonian parameters were obtained by simulation of the spectra with XSophe [58,59].

Table 2
dd-transitions of the divalent transition metal complexes of the bisdipyrazole-based ligand $\mathbf{L}^3$ in comparison with the Cu^{II} complexes of the hexadentate ligands $\mathbf{L}^1$ and $\mathbf{L}^2$.

Compound	dd transitions solution (nm)	dd transitions solid (nm)
$[Fe\mathbf{L}^3]^{2+}$	835 (max), 960 (sh)	830 (max), 1010
$[Co\mathbf{L}^3]^{2+}$	480 (max), 950, 1040 (sh)	475 (max), 940, 1060
$[Ni\mathbf{L}^3]^{2+}$	520, 640, 800 (sh), 960 (max)	530, 650, 820 (sh), 970 (max)
$[Cu\mathbf{L}^3]^{2+}$	650 (max), 900 (sh)	670 (max), 890 (sh)
$[Cu\mathbf{L}^1]^{2+}$[a]	620	
$[Cu\mathbf{L}^2]^{2+}$[b]	622	

[a] Ref. [36].
[b] Ref. [35].

3.2. Syntheses

3.2.1. Compound **3** ($C_{16}H_{15}NO_4$; 285.29 g/mol)

1,8-Naphthalic acid anhydride (19.82 g, 0.1 mol, 1.0 equiv) and 1-aminoacetaldehyde-dimethylacetal (12.49 g, 12.94 ml, 0.12 mol, 1.2 equiv) were dissolved in 250 ml of ethanol and heated to reflux for 4 h. After allowing the reaction mixture to cool to room temperature a brown solid precipitated. This brown solid was filtrated and washed with ethanol (3 × 200 ml) to afford long white needles as the pure product in a yield of 88.4% (25.22 g, 88.4 mmol). ^{1}H NMR (400 MHz, $CDCl_3$): $\delta = 3.42$ (s, 6H, OCH_3), 4.40 (d, $J = 5.65$ Hz, 2H, $NCH_2CH(OMe)_2$), 4.92 (t, $J = 5.65$ Hz, 1H, $NCH_2CH(OMe)_2$), 7.76 (t, $J = 7.78$ Hz, 2H, H_{naph}), 8.22 (d, $J = 8.16$ Hz, 2H, H_{naph}), 8.61 (d, $J = 7.40$ Hz, 2H, H_{naph}). ^{13}C NMR (100 MHz, $CDCl_3$): $\delta = 40.82$, 53.45, 100.58, 122.49, 126.91, 128.22, 131.39, 131.55, 134.00, 164.24. HR-ESI (pos): $[M+Na]^+$ calc. 308.08988, obs. 308.08908; $[2M+Na]^+$ calc. 593.18999, obs. 593.18918. Elemental analysis (Report No.: 29570): [M] calc. C, 67.36; H, 5.30; N, 4.91; obs. C, 67.11; H, 5.35; N, 4.89%.

3.2.2. Compound **4** ($C_{20}H_{15}N_5O_2$; 357.37 g/mol)

2-(2,2-Dimethoxyethyl)-1H-benzo[d,e]isoquinoline-1,3(2H)-dione (24.2 g, 84.83 mmol, 1.0 equiv), pyrazole (17.3 g, 254.11 mmol, 3.0 equiv) and *para*-toluene sulfonic acid monohydrate (350 mg) were heated to 220 °C for 4 h in a distillation apparatus in order to get rid of the resulting methanol. After allowing the reaction mixture to cool to room temperature the brownish product crystallized. The solid was suspended in 300 ml of dichloromethane, filtrated and mortared. The solid was then washed with 1 l of a saturated K_2CO_3-solution and 1 l of water. The remaining solid was dried under high vacuum to afford a light brown solid as the pure product in a yield of 87.85% (26.63 g, 74.52 mmol). ^{1}H NMR (400 MHz, $CDCl_3$): δ = 5.30 (d, *J* = 7.28 Hz, 2H, CH_2CH(pz)$_2$), 6.27 (t, *J* = 2.01 Hz, 2H, H$^{4'}$), 7.17 (t, *J* = 7.28 Hz, 1H, CH$_2$C*H*(pz)$_2$), 7.49 (d, *J* = 1.25 Hz, 2H, H$^{3'}$), 7.73 (t, *J* = 7.72 Hz, 2H, H$_{naph}$), 7.85 (d, *J* = 2.38 Hz, 2H, H$^{5'}$), 8.20 (d, *J* = 8.16 Hz, 2H, H$_{naph}$), 8.56 (d, *J* = 7.28 Hz, 2H, H$_{naph}$). ^{13}C NMR (100 MHz, $CDCl_3$): δ = 42.40, 72.04, 106.70, 121.97, 126.92, 128.20, 129.56, 131.53, 131.61, 134.31, 140.26, 163.94. HR-ESI (pos): [M+H]$^+$ calc. 358.13040, obs. 358.12980; [M+Na]$^+$ calc. 380.11234, obs. 380.11175; [M+K]$^+$ calc. 396.08628, obs. 396.08571; [2M+H]$^+$ calc. 737.23492, obs. 737.23340. Elemental analysis (Report No.: 29569): [M] calc. C, 67.22; H, 4.23; N, 19.60; obs. C, 66.93; H, 4.26; N, 19.38%.

3.2.3. Compound **5** ($C_8H_{11}N_5$; 177.21 g/mol)

2-(2,2-Dipyrazol-1-yl-ethyl)-benzo[d,e]iso-quinoline-1,3-dione (30.72 g, 85.96 mmol, 1.0 equiv) was suspended in 200 ml of warm toluene. Then hydrazine monohydrate (31.9 g, 31.0 ml, approx. 1.0 mol, approx. 10.0 equiv) was added and this suspension was refluxed over night whereupon a yellow precipitate formed. The suspension was allowed to cool to room temperature and excess of hydrazine hydrate and toluene were removed by a rotary evaporator. In order to extract the free amine the precipitate was washed with water (4 × 50 ml). The aqueous solution was concentrated under high vacuum to afford an oily brown solid as the pure product in a quantitative yield. ^{1}H NMR (400 MHz, $CDCl_3$): δ = 1.67 (br. s, 2H, NH_2), 3.77 (d, *J* = 7.03 Hz, 2H, CH_2CH(pz)$_2$), 6.30 (t, *J* = 2.13 Hz, 2H, H$^{4'}$), 6.36 (t, *J* = 6.96 Hz, 1H, CH$_2$C*H*(py)$_2$), 7.58 (d, *J* = 1.63 Hz, 2H, H$^{3'}$), 7.60 (d, *J* = 2.38 Hz, 2H, H$^{5'}$). ^{13}C NMR (100 MHz, $CDCl_3$): δ = 44.93, 77.37, 106.66, 128.94, 140.33. HR-FAB (pos): [M+H]$^+$ calc. 178.1093, obs. 178.1090. Elemental analysis (Report No.: 29202): [M+1/5H_2O] calc. C, 53.14; H, 6.36; N, 38.73; obs. C, 53.31; H, 6.26; N, 38.46%.

3.2.4. **L^3** ($C_{35}H_{36}N_{10}O$; 612.73 g/mol)

1,3-Diphenyl-2-propanone (3.56 g, 16.93 mmol, 1.0 equiv), paraformaldehyde (2.03 g, 67.72 mmol, 4.0 equiv) and acetic acid (5.08 g, 4.84 ml, 84.65 mmol, 5.0 equiv) were mixed in 100 ml of ethanol and slowly heated to 60 °C. At this temperature 2,2-di(1*H*-pyrazol-1-yl)ethanamine (6.00 g, 33.86 mmol, 2.0 equiv) was added to the reaction mixture and heated to reflux over night. The solution was allowed to cool to room temperature whereupon a pale yellow precipitate formed which was filtrated and washed with ethanol to afford a white solid as the product in a yield of 44.36% (4.60 g, 7.51 mmol). Crystals suitable for X-ray diffraction were obtained by recrystallization from acetonitrile. ^{1}H NMR (400 MHz, $CDCl_3$): δ = 3.17 (d, *J* = 10.67 Hz, 4H, CH_{ax}H$_{eq}$), 3.36 (d, *J* = 10.67 Hz, 4H, CH$_{ax}$$H_{eq}$), 3.61 (d, *J* = 7.40 Hz, 4H, CH_2CH(pz)$_2$), 6.33 (t, *J* = 2.07 Hz, 4H, H$^{4'}$), 6.53 (t, *J* = 7.40 Hz, 2H, C*H*(pz)$_2$), 6.93 (d, *J* = 7.03 Hz, 4H, Ph), 7.20–7.31 (m, 6H, Ph), 7.58 (d, *J* = 1.51 Hz, 4H, H$^{3'}$), 7.67 (d, *J* = 2.26 Hz, 4H, H$^{5'}$). ^{13}C NMR (100 MHz, $CDCl_3$): δ = 54.27, 58.58, 65.00, 73.41, 106.81, 126.55, 126.78, 127.97, 128.90, 140.19, 142.00, 209.74. HR-ESI (pos): [M+H]$^+$ calc. 613.31518, obs. 613.31452; [M+Na]$^+$ calc. 635.29713, obs. 635.29697; [M+K]$^+$ calc. 651.27106; obs. 651.27115. Elemental analysis (Report No.: 30169): [M] calc. C, 68.61; H, 5.92; N, 22.86; obs. C, 68.57; H, 6.11; N, 22.74%.

3.2.5. [Fe^{II}L^3][ClO$_4$]$_2$

To a solution of the ligand **L**^{3} (0.2 mmol, 122.5 mg, 1.0 equiv) in 2.5 ml of acetonitrile was added $Fe(ClO_4)_2\cdot 10H_2O$ (0.2 mmol, 87.0 mg, 1.0 equiv) dissolved in 2.5 ml of acetonitrile. This solution was stirred at room temperature over night. Pale brown needles were obtained by ether diffusion of this solution at room temperature in a yield of 50.0% (85.9 mg, 0.10 mmol). HR-ESI (pos): [Fe^{II}**L**^{3}+ClO$_4$$^-$]$^+$ calc. 767.19081, obs. 767.19303. Elemental analysis (Report No.: IPMB24): [Fe**L**^{3}(ClO$_4$)$_2$.H$_2$O] calc. C, 47.47; H, 4.33; N, 15.82; obs. C, 47.06; H, 4.47; N, 15.62%.

3.2.6. [Co^{II}L^3][ClO$_4$]$_2$

To a solution of the ligand **L**^{3} (0.2 mmol, 122.5 mg, 1.0 equiv) in 2.5 ml of acetonitrile was added $Co(ClO_4)_2\cdot 6H_2O$ (0.2 mmol, 73.19 mg, 1.0 equiv) dissolved in 2.5 ml of acetonitrile. This solution was stirred at room temperature over night. The solution was then stored at −18 °C for several days. The solution was then freed from white solid material that precipitated and subjected to ether diffusion at room temperature. A red crystalline solid was obtained in a yield of 70.0% (117.9 mg, 0.14 mmol). HR-ESI (pos): [L^3+Co]$^{2+}$ calc. 335.62028, obs. 335.61996. Elemental analysis (Report No.: IPMB21): [Co**L**^{3}(ClO$_4$)$_2$·CH$_3$CN] calc. C, 48.75; H, 4.31; N, 16.90; obs. C, 49.43; H, 4.76; N, 16.24%.

3.2.7. [Ni^{II}L^3][ClO$_4$]$_2$

To a solution of the ligand **L^3** (0.2 mmol, 122.5 mg, 1.0 equiv) in 2.5 ml of acetonitrile was added $Ni(ClO_4)_2\cdot 6H_2O$ (0.2 mmol, 73.1 mg, 1.0 equiv) dissolved in 2.5 ml of acetonitrile. This solution was stirred at room temperature over night. Pink needles were obtained by ether diffusion of this solution at 2 °C in a yield of 50.0% (91.0 mg, 0.10 mmol). HR-ESI (pos): [Ni^{II}**L**^{3}ClO$_4$$^-$]$^+$ calc. 769.19121, obs. 769.19475. Elemental analysis (Report No.: 30092): [Ni**L**^{3}(ClO$_4$)$_2$·0.5H$_2$O] calc. C, 47.81; H, 4.24; N, 15.93; obs. C, 47.81; H, 4.05; N, 15.92%.

3.2.8. [Cu^{II}L^3][BF$_4$]$_2$

To a solution of the ligand **L**^{3} (0.2 mmol, 122.5 mg, 1.0 equiv) in 2.5 ml of acetonitrile was added dry $Cu(BF_4)_2$ (0.2 mmol, 47.5 mg, 1.0 equiv) dissolved in 2.5 ml of acetonitrile. This solution was stirred at room temperature over night. Blue needles were obtained by ether diffusion of this solution at room temperature in a yield of 50.0% (81.9 mg, 0.10 mmol). HR-ESI (pos): [Cu^{II}+**L**^{3}+BF$_4$]$^+$ calc. 762.23988, obs. 762.23994. Elemental analysis (Report No.: 29745): [Cu**L**^{3}(BF$_4$)$_2$·2H$_2$O] calc. C, 47.45; H, 4.55; N, 15.81; obs. C, 47.73; H, 4.66; N, 15.91%.

3.2.9. [Zn^{II}L^3][ClO$_4$]$_2$

To a warm solution of the ligand **L^3** (0.2 mmol, 122.5 mg, 1.0 equiv) in 2.5 ml of acetonitrile was added $Zn(ClO_4)_2\cdot 6H_2O$ (0.2 mmol, 74.5 mg, 1.0 equiv) in 2.5 ml of warm acetonitrile. The resulting suspension was stirred at room temperature over night and afterwards stored at −18 °C. The solution was removed from the precipitate and separately allowed to stand at room temperature whereupon the solvent slowly evaporated. Colorless crystals were obtained in a yield of 45.0% (80.0 mg, 0.09 mmol). Elemental analysis (Report No.: 30091): [Zn**L**^{3}(ClO$_4$)$_2$·2H$_2$O] calc. C, 46.04; H, 4.42; N, 15.34; obs. C, 45.90; H, 4.36; N, 15.21%.

Acknowledgments

Generous financial support by the German Science Foundation (DFG) and the University of Heidelberg is gratefully acknowledged.

Appendix A. Supplementary data

CCDC 878253–878258 contains the supplementary crystallographic data for this paper. These data can be obtained free of charge via http://www.ccdc.cam.ac.uk/conts/retrieving.html, or from the Cambridge Crystallographic Data Centre, 12 Union Road, Cambridge CB2 1EZ, UK; fax: (+44) 1223-336-033; or e-mail: deposit@ccdc.cam.ac.uk. Supplementary data associated with this article can be found, in the online version, at http://dx.doi.org/10.1016/j.poly.2012.06.035.

References

[1] R.J. Gisbert, Coordination Chemistry, Wiley-VCH, 2008.
[2] M. Gerloch, E.C. Constable, Transition Metal Chemistry – The Valence Shell in D-Bloch Chemistry, VCH, 1994.
[3] M. Gerloch, Coord. Chem. Rev. 99 (1990) 199.
[4] P. Comba, M. Kerscher, Coord. Chem. Rev. 253 (2009) 564.
[5] K. Seppelt, Acc. Chem. Res. 36 (2003) 147.
[6] P. Comba, Coord. Chem. Rev. 182 (1999) 343.
[7] R.G. Dickinson, L. Pauling, J. Am. Soc. 45 (1923) 466.
[8] R. Hultgren, Phys. Rev. 40 (1923) 891.
[9] R. Eisenberg, J.A. Ibers, Inorg. Chem. 5 (1966) 411.
[10] R. Eisenberg, Prog. Inorg. Chem. 12 (1970) 295.
[11] W.O. Gillum, R.A.D. Wentworth, R.F. Childers, Inorg. Chem. 9 (1970) 1825.
[12] A.A.G. Tomlinson, J. Chem. Soc. A (1971) 1409.
[13] R.A.D. Wentworth, Coord. Chem. Rev. 9 (1972) 171.
[14] E. Larsen, G.N. La Mar, B.E. Wagner, J.E. Parks, R.H. Holm, Inorg. Chem. 11 (1972) 2652.
[15] J.K. Burdett, Inorg. Chem. 15 (1976) 212.
[16] R. Hoffmann, J.M. Howell, A.R. Rossi, J. Am. Chem. Soc. 98 (1976) 2484.
[17] A. Avdeef, J.A. Costamagna, J.P. Fackler, Inorg. Chem. 13 (1974) 1854.
[18] D.L. Kepert, Inorganic Chemistry Concepts, vol. 6, Springer-Verlag, Berlin, Heidelberg, New York, 1980.
[19] P. Comba, L.M. Engelhardt, J.M. Harrowfield, E. Horn, A.M. Sargeson, M.R. Snow, A.H. White, Inorg. Chem. 24 (1985) 2325.
[20] P. Comba, Inorg. Chem. 28 (1989) 426.
[21] P. Comba, T.W. Hambley, M. Ströhle, Helv. Chim. Acta 78 (1995) 2042.
[22] R.J. Deeth, Coord. Chem. Rev. 212 (2001) 11.
[23] A. Bentz, P. Comba, R.J. Deeth, M. Kerscher, H. Pritzkow, B. Seibold, H. Wadepohl, Inorg. Chem. 47 (2008) 9518.
[24] B.N. Figgis, M.A. Hitchman, Ligand Field Theory and Its Applications, Wiley-VCH, Weinheim, New York, 2000.
[25] P. Comba, A.F. Sickmüller, Inorg. Chem. 36 (1997) 4500.
[26] D. Banerjea, J.C. Bailar Jr., Transition Met. Chem. 10 (1985) 331.
[27] C. Mannich, P. Mohs, Chem. Ber. B63 (1930) 608.
[28] H. Stetter, R. Merten, Chem. Ber. 90 (1957) 868.
[29] R. Haller, Arch. Pharm. 302 (1969) 113.
[30] P. Comba, A. Lienke, Inorg. Chem. 40 (2001) 5206.
[31] P. Comba, M. Kerscher, M. Merz, V. Müller, H. Pritzkow, R. Remenyi, W. Schiek, Y. Xiong, Chem. Eur. J. 8 (2002) 5750.
[32] P. Comba, W. Schiek, Coord. Chem. Rev. 238–239 (2003) 21.
[33] P. Comba, M. Kerscher, W. Schiek, Prog. Inorg. Chem. 55 (2007) 613.
[34] P. Comba, C. Lopez de Laorden, H. Pritzkow, Helv. Chim. Acta 88 (2005) 647.
[35] P. Comba, C. Haaf, H. Wadepohl, Inorg. Chem. 48 (2009) 6604.
[36] C. Bleiholder, H. Börzel, P. Comba, R. Ferrari, A. Heydt, M. Kerscher, S. Kuwata, G. Laurenczy, G.A. Lawrance, A. Lienke, B. Martin, M. Merz, B. Nuber, H. Pritzkow, Inorg. Chem. 44 (2005) 8145.
[37] K. Born, P. Comba, R. Ferrari, S. Kuwata, G.A. Lawrance, H. Wadepohl, Inorg. Chem. 46 (2007) 458.
[38] P. Comba, C. Lang, C. Lopez de Laorden, A. Muruganantham, G. Rajaraman, H. Wadepohl, M. Zajaczkowski, Chem. Eur. J. 14 (2008) 5313.
[39] J. Madhavan, P. Comba, M. Maurer, P. Vadivelu, V. Venuvanalingham, Dalton Trans. 40 (2011) 11276.
[40] M.R. Bukowski, P. Comba, A. Lienke, C. Limberg, C. Lopez de Laorden, R. Mas-Balleste, M. Merz, L. Que Jr., Angew. Chem., Int. Ed. 45 (2006) 3446.
[41] P. Comba, M. Maurer, P. Vadivelu, Inorg. Chem. 48 (2009) 10389.
[42] P. Comba, S. Wunderlich, Chem. Eur. J. 16 (2010) 7293.
[43] D.L. Reger, R.F. Seminiuc, J.R. Gardinier, J. O'Neal, B. Reinecke, M.D. Smith, Inorg. Chem. 45 (2006) 4337.
[44] H. Börzel, P. Comba, C. Katsichtis, W. Kiefer, A. Lienke, V. Nagel, H. Pritzkow, Chem. Eur. J. 5 (1999) 1716.
[45] H. Börzel, P. Comba, K.S. Hagen, M. Kerscher, H. Pritzkow, M. Schatz, S. Schindler, O. Walter, Inorg. Chem. 41 (2002) 5440.
[46] H. Börzel, P. Comba, H. Pritzkow, J. Chem. Soc., Chem. Commun. (2001) 97.
[47] K. Born, P. Comba, A. Daubinet, A. Fuchs, H. Wadepohl, J. Biol. Inorg. Chem. 12 (2007) 36.
[48] P. Comba, B. Martin, A. Muruganantham, J. Straub, Inorg. Chem., submitted for publication.
[49] P. Comba, C. Haaf, S. Helmle, K.D. Karlin, S. Pandian, A. Waleska, Inorg. Chem. 51 (2012) 2841.
[50] P. Comba, M. Merz, H. Pritzkow, Eur. J. Inorg. Chem. (2003) 1711.
[51] P. Comba, C. Haaf, A. Lienke, A. Muruganantham, H. Wadepohl, Chem. Eur. J. 15 (2009) 10880.
[52] S. Juran, M. Walther, H. Stephan, R. Bergmann, J. Steinbach, W. Kraus, F. Emmerling, P. Comba, Bioconjugate Chem. 20 (2009) 347.
[53] E.A. Ambundo, M.-V. Deydier, A.J. Grall, N. Agnera-Vega, L.T. Dressel, T.H. Cooper, N.J. Heeg, L.A. Ochrymowycz, D.B. Rorabacher, Inorg. Chem. 38 (1999) 4233.
[54] D.D. Perrin, B. Dempsey, Buffers for pH and Metal Ion Control, Chapman and Hall Ltd., London, New York, 1974.
[55] T. Astley, A.J. Canty, M.A. Hitchman, G.L. Rowbottom, B.W. Skelton, A.H. White, J. Chem. Soc., Dalton Trans. (1991) 1981.
[56] P. Comba, B. Martin, A. Prikhod'ko, H. Pritzkow, H. Rohwer, C. R. Chim. 6 (2005) 1506.
[57] P.V. Bernhardt, P. Comba, Inorg. Chem. 32 (1993) 2798.
[58] D. Wang, G.R. Hanson, J. Magn. Reson. A 117 (1995) 1.
[59] D. Wang, G.R. Hanson, Appl. Magn. Reson. 11 (1996) 401.